Anomalous angular distribution of fragment ions from rare-gas diatomic molecules with intense, femtosecond, near-infrared laser pulses

Shinichirou Minemoto* and Hirofumi Sakai†

Department of Physics, Graduate School of Science, The University of Tokyo, 7-3-1, Hongo, Bunkyo-ku, Tokyo 113-0033, Japan

(Received 21 December 2006; published 23 March 2007)

Almost isotropic angular distributions are observed for fragment ions from Xe_2 produced with intense femtosecond laser pulses (800 nm, 4×10^{14} W/cm^2). The results observed for Xe_2 present a great contrast to those for I_2 molecules used as reference molecules, which show typical anisotropic angular distributions resulting from enhanced ionization. The kinetic energy spectra of the fragment ions from Xe_2 reveal that the internuclear distance remains near the equilibrium distance for various pulse widths from 45 to 710 fs, indicating that in the rising edge of the pulses, the internuclear distance of Xe_2^{n+} (n=0, 1, 2) does not reach the favorable region for enhanced ionization even though enhancement can potentially work for Xe_2^{n+}. The dynamic alignment of neutral Xe_2 during the pulses is also discussed on the basis of numerical simulations.

DOI: 10.1103/PhysRevA.75.033413 PACS number(s): 33.80.Rv, 33.80.Wz

I. INTRODUCTION

Multiphoton ionization of molecules is one of the fundamental processes observed in the interaction with intense laser pulses. It is well known that a molecule subjected to an intense visible-infrared laser pulse is dissociatively ionized and produces fragment ions preferentially along the laser polarization direction [1,2]. The anisotropic distribution of the fragment ions produced from multiply charged parent ions is interpreted by any of the dynamic (nonadiabatic) alignment of molecules or their ions [3], the angle-dependent ionization rate (enhanced ionization) [4–9], and the combination of both mechanisms. For example, in the case of halogen diatomic molecules irradiated by an intense pulse with the same intensity [10], what determines the dominant mechanism is the mass of the constituent atoms. Lighter molecules such as Cl_2 can be dynamically aligned during the dissociative ionization with an 80 fs pulse, while the anisotropic distribution observed for heavier molecules such as I_2 can be attributed mainly to enhanced ionization. In enhanced ionization, the internuclear distance of molecules is elongated at the rising edge of an intense laser pulse and, when the distance reaches around a critical region which is typically twice as long as the equilibrium distance R_{eq}, molecules that happen to align along the laser polarization direction are much more easily ionized than those orienting other directions. As a result of enhanced ionization, the fragment ions produced from multiply charged parent ions are distributed more along the laser polarization direction and their kinetic energies are usually smaller than the Coulomb repulsion energies at R_{eq}. In either mechanism, the anisotropy of fragment ions should become more distinct for pulses with longer widths because the nuclei in a molecule can have more time to align along the polarization direction (dynamic alignment) or to reach the critical internuclear distance (enhanced ionization).

However, rather surprising results were observed in our recent studies [11]. The fragment ions produced from rare-gas diatomic molecules Rg_2 (Rg: from lighter Ar to heavier Xe) with 45 fs infrared laser pulses show isotropic distribution, which is not compatible either with the dynamic alignment or with enhanced ionization. Our observations are also incompatible with recent time-dependent density functional calculations [9], predicting that, also for Ne_2 in the same series of Rg_2, ionization rates are enhanced at a critical distance of around or slightly longer than R_{eq} through a mechanism analogous to enhanced ionization. In this paper, what is happening in the multiphoton ionization of Xe_2 is elucidated by measuring the kinetic energies and the angular distributions of fragment ions as a function of the pulse width of ionization laser pulses. We investigate the effect of enhanced ionization together with that of dynamic alignment of neutral molecules by using I_2 molecules as a reference, which have a similar mass to that of Xe_2 and is expected to show a similar behavior of dynamic alignment for a given pulse width.

II. EXPERIMENT

Here, an outline of the experiments is described and the details are found in our recent papers [11–14]. Figure 1 shows the schematic diagram of our experimental setup. The molecular samples are prepared by the supersonic expansion of sample gas mixtures with the total pressure of 1 atm through a pulsed valve with a diameter of 0.5 mm. For I_2, a room-temperature I_2 buffered with Ar is used as the sample gas. For Xe_2, a gas mixture of 5% Xe in Ar is used. In these conditions, larger clusters (I_2Ar_n with $n\geq1$ and Xe_n with $n\geq3$) are confirmed to be negligible compared to I_2 and Xe_2. As shown in the inset of Fig. 1, the intensity of Xe_2^+ ions is in the order of 0.1% that of Xe^+ and that of Xe_3^+ is negligible. After passing through two 0.5 mm skimmers, the sample beam is introduced into the interaction region with the ionization pulses.

The molecules are ionized by intense femtosecond pulses from the Ti:sapphire based chirped pulse amplified (CPA) system (Spectra-Physics, Super Spitfire). The pulse has the center wavelength of ~800 nm with a bandwidth of ~16 nm. The pulse width is adjusted by changing the degree of chirp with the compressor in the CPA system. The pulse

*Electronic address: minemoto@phys.s.u-tokyo.ac.jp
†Electronic address: hsakai@phys.s.u-tokyo.ac.jp

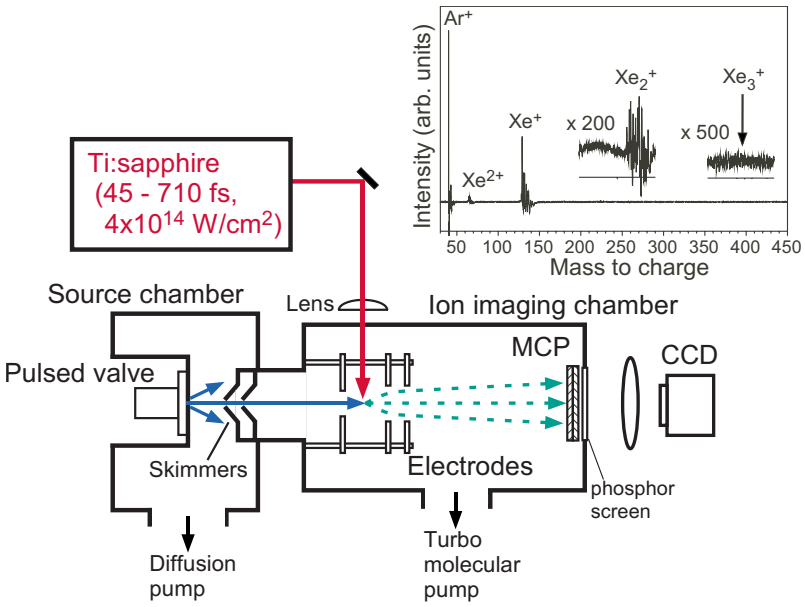

FIG. 1. (Color online) Schematic diagram of the experimental setup. The inset shows a typical time-of-flight spectrum obtained by irradiating the femtosecond pulses into the Xe/Ar mixture.

width τ is measured by a homemade SHG-FROG (Frequency Resolved Optical Gating) system. The shortest pulse width is $\tau \sim 45$ fs. We use only the negatively chirped pulses because their amplitude profiles are less structured than those of positively chirped pulses. It is confirmed that no difference is made in the fragment distributions by the negatively and the positively chirped pulses with the same pulse widths. The (elongated) femtosecond pulses are focused by a plano-convex lens ($f=300$ mm) to a spot size of $\omega_0 \sim 13$ μm. The peak intensity is kept constant by adjusting the output energy from the CPA system. The maximum peak intensity used is estimated to be $\sim 4 \times 10^{14}$ W/cm^2.

The fragment ions produced are analyzed by the velocity map ion imaging technique [15]. They are detected by a microchannel plate (MCP) backed by a phosphor screen. A homemade power supply provides the MCP with a pulsed high voltage in order to gate the desired ions with a specific mass-to-charge ratio. The two-dimensional (2D) ion images on the phosphor screen are recorded by a charge-coupled device camera and are transferred to and stored in a personal computer by a homemade software. The three-dimensional fragment distribution is reconstructed from the obtained 2D images by an iterative Abel inversion technique [16]. The kinetic energy of the fragment ions is calibrated on the basis of the precise measurements of their time of flight. An error associated with the absolute value of the kinetic energy is typically ±3%.

III. RESULTS AND DISCUSSIONS

Figure 2(a) shows the Abel inverted image of I^+ from I_2 exposed to the ultrashort pulses of $\tau=45$ fs. The polarization direction is shown by the arrow. The intense center signals in the image are attributed to the molecular dications I_2^{2+}. Apart from the center signals, there appear three rings. Considering the kinetic energy of the fragment ions, these rings can be attributed to the channels $I^+ + I$ from I_2^+, $I^+ + I^+$ from I_2^{2+}, and $I^+ + I^{2+}$ from I_2^{3+} from the inner to the outer rings, respectively. The rings show a slight anisotropy, i.e., the fragment ions are likely to be observed along the laser polarization direction. The anisotropy can be understood by the enhanced ionization mechanism as explained above. As shown in Figs.

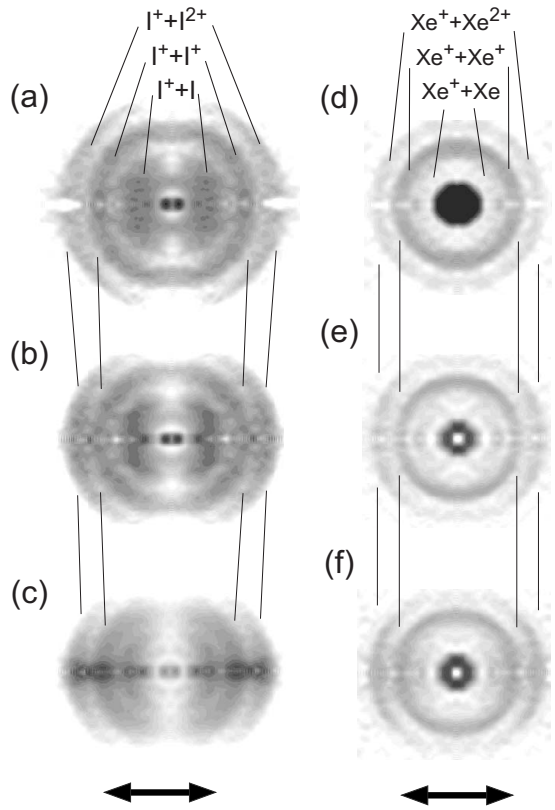

FIG. 2. Abel inverted images of [(a)–(c)] I^+ from I_2^{n+} ($n=1-3$) and [(d)–(f)] Xe^+ from Xe_2^{n+} ($n=1-3$). The polarization directions are shown by the arrows. The pulse widths of the ionization pulses are (a) 45, (b) 290, (c) 660, (d) 45, (e) 320, and (f) 710 fs. The solid lines trace the densest positions of dissociative ionization channels to guide the eye.

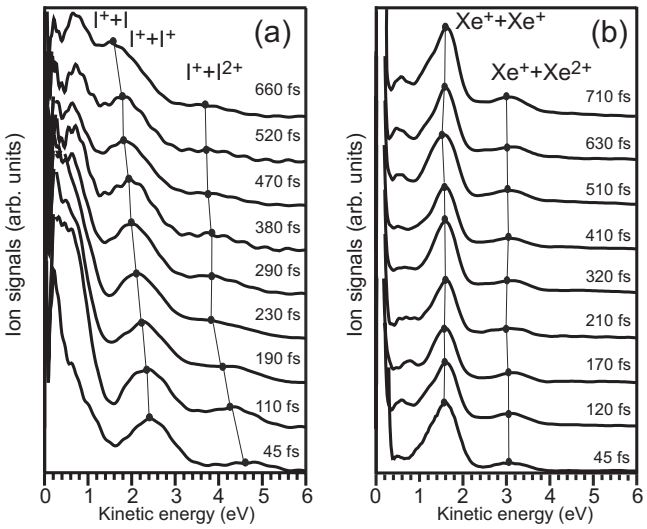

FIG. 3. Kinetic energy spectra of (a) I^+ and (b) Xe^+ ions obtained by angularly integrating the Abel inverted images. The labels show the pulse widths τ's. The dots represent the weighted peak positions of dissociative ionization channels $A^+ + A^+$ and $A^+ + A^{2+}$ (A=I and Xe) obtained by the least-squares fit assuming Gaussian profiles (see text).

2(a)–2(c), the anisotropy becomes more distinct by increasing the pulse width τ from 45 to 660 fs. We also note that the outer two rings corresponding to the dissociation channels from I_2^{2+} and I_2^{3+} shrink as τ's are increased. This means that the kinetic energy released from the potential energy is decreased as τ is increased. If most of the excited states of I_2^{2+} and I_2^{3+} have repulsive potentials, which approach the pure Coulombic potential at large internuclear distance ($R \geq 5$ Å) [17], the observed shrink of the outer two rings also means that, as τ is increased, the internuclear distance is elongated in the course of the production of multiply charged molecular ions till the explosive dissociation takes place as discussed below.

On the other hand, Xe^+ ions from Xe_2 behave in a quite different way as shown in Figs. 2(d)–2(f). The intense center signals are Xe^+ ions produced by the ionization of neutral Xe atoms. All the three rings corresponding to $Xe^+ + Xe$, $Xe^+ + Xe^+$, and $Xe^+ + Xe^{2+}$ channels are rather isotropic and the constituent atoms behave as if they were independent of the polarization direction of the laser pulses. Furthermore, the change in the Xe^+ images with the pulse width τ is inappreciable. The outer rings corresponding to the dissociation channels from Xe_2^{2+} and Xe_2^{3+} do not shrink and do not show distinct anisotropy along the polarization direction as τ is increased. These observations show that neither enhanced ionization nor dynamic alignment plays a significant role in the multiple ionization processes of Xe_2.

Figure 3 shows the kinetic energy spectra of (a) I^+ and (b) Xe^+ ions obtained by angularly integrating the Abel inverted images. The spectra are labeled by the pulse widths τ's. The multiple peaks in the spectra of I^+ and Xe^+ correspond to the three rings in the ion images. The small-energy peaks, at ~0.2 and ~0.7 eV for I^+ and at ~0.5 eV for Xe^+, are located at the same position irrespective of τ. These peaks can be attributed to the photodissociation channels $A^+ + A$ (A=I and Xe) from singly charged parent ions A_2^+. Two photodissociation peaks observed in the I^+ spectra are due to two different photodissociation channels accompanied by the lower and higher electronic states of the atom. The fragment ions from the $I(^2P_{3/2}) + I(^2P_{1/2})$ channel have smaller kinetic energy by 0.5 eV than those from the $I(^2P_{3/2}) + I(^2P_{3/2})$ channel.

The middle- and the highest-energy peaks in the kinetic energy spectra can be attributed to the dissociative ionization channels from multiply charged parent ions, i.e., $A^+ + A^+$ from A_2^{2+} and $A^+ + A^{2+}$ from A_2^{3+}, respectively. We least squares fit the peaks in the kinetic energy spectra by assuming Gaussian profiles. The solid dots in Fig. 3 show the weighted centers thus obtained for the $A^+ + A^+$ and $A^+ + A^{2+}$ channels. In the spectra of I^+ ions at τ=45 fs, the weighted centers of $I^+ + I^+$ and $I^+ + I^{2+}$ channels are 2.5 and 4.6 eV, respectively. The peaks of dissociative ionization channels shift to lower kinetic energies as τ is increased. The monotonic decrease of the kinetic energy of the fragment ions ensures that the potentials relevant to the dissociative ionization are repulsive [18]. In such a case, the decreased kinetic energy of the fragment ions corresponds to the elongation of the internuclear distance at which the explosive dissociation takes place immediately after the production of multiply charged molecular ions. The results shown in Fig. 3(a) show that this is the case for the multiphoton ionization processes in I_2. In fact, the weighted centers of $I^+ + I^+$ and $I^+ + I^{2+}$ channels at τ=45 fs decrease as τ is increased and come down to 1.6 and 3.6 eV at τ=660 fs, which are 64% and 78% of those at τ=45 fs, respectively.

In the kinetic energy spectra of Xe^+ ions obtained with 45 fs pulses [Fig. 3(b)], the peaks centered at 1.6 and 3.1 eV correspond to the $Xe^+ + Xe^+$ and $Xe^+ + Xe^{2+}$ channels, respectively. However, in contrast to the I_2 case, the weighted centers of $Xe^+ + Xe^+$ and $Xe^+ + Xe^{2+}$ channels do not move with τ. Based on the same logic as used above, unchanged kinetic energies observed in Fig. 3(b) mean that the internuclear distance remains the same for the pulse widths of 45–710 fs.

The remarkable difference between I_2 and Xe_2 in the τ dependence of the kinetic energy spectra can be understood by the difference in the densities of electronic excited states in the lower energy regions. In Fig. 4, plausible multiphoton ionization processes in (a) I_2 and (b) Xe_2 are shown together with the ground and some low-lying potentials for neutral and singly charged molecules. In the case of I_2 [Fig. 4(a)], there are more than 10 electronic excited states below 3.1 eV (accessible with 2 photons) at R_{eq} and most of them have repulsive or shallow potentials [19]. Iodine molecules subjected to the rising edge of intense laser pulses will be excited to some of these low-lying excited states with one or two photons and start to dissociate until they are multiply ionized and explosively dissociate. With the pulses of τ =45 fs, I_2 molecules are multiply ionized right after the excitation and hence the fragment ions have the largest kinetic energy released from the sum of the dominant ionic potentials and the small energies from dissociation. As τ is increased, I_2 molecules can spend more time to elongate their internuclear distance before multiple ionization on repulsive potentials and accordingly the kinetic energies of fragment ions become smaller because the energies released from ionic potentials are also decreased.

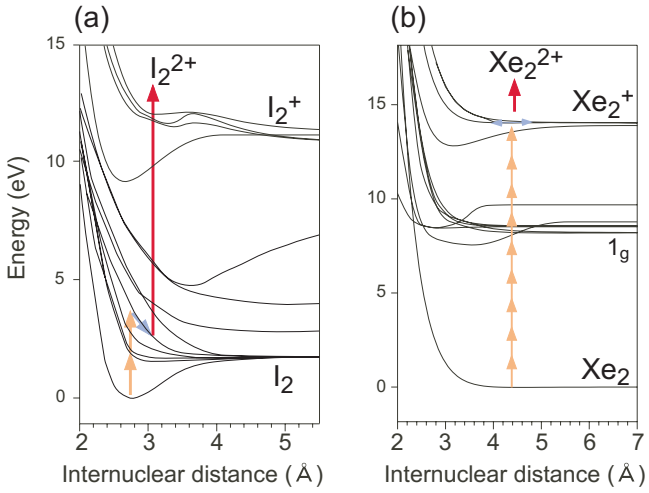

FIG. 4. (Color online) Plausible multiphoton ionization processes in (a) I_2 and (b) Xe_2 together with the ground and some low-lying potentials for neutral and singly charged molecules (see text). The potentials for I_2 and Xe_2 are taken from Ref. [19] and Refs. [20–22,31,32], respectively.

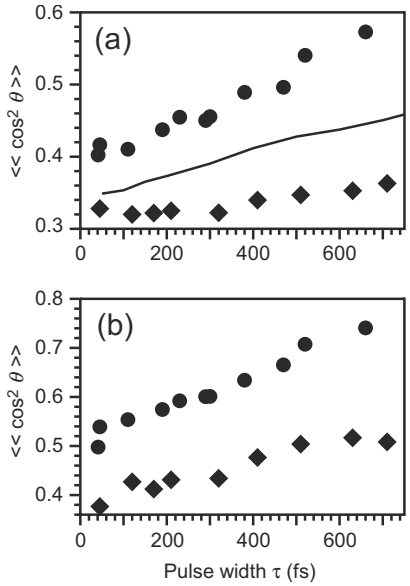

FIG. 5. The pulse width dependence of the anisotropy parameter $\langle\langle\cos^2\theta\rangle\rangle$ for the channels of (a) $A^+ + A^+$ (A=I and Xe) and (b) $A^+ + A^{2+}$. The solid circles and diamonds represent $\langle\langle\cos^2\theta\rangle\rangle$ obtained for I^+ and Xe^+, respectively. The solid curve in (a) shows the upper limit of the dynamic alignment, namely $\langle\langle\cos^2\theta\rangle\rangle_{ul}$ calculated for neutral Xe_2 (see text).

The above scenario, however, cannot be applied to the multiphoton ionization processes in Xe_2 [Fig. 4(b)]. The lowest excited state of Xe_2 ($^3\Sigma_u^+$) lies ~8 eV above the ground state [20], which is characteristic of rare-gas diatomic molecules, and at least 6 photons are required for Xe_2 to be excited. It is unlikely that Xe_2 absorbs so many photons in the less intense rising edge of the pulses and elongates the internuclear distance. Rather, Xe_2^+ would be produced slightly before the peak of the pulse. Once Xe_2^+ are produced, their internuclear distance might be changed in the excited states. However, as shown in Fig. 4(b), the potentials of the excited states are rather flat in the vicinity of the Franck-Condon region of the equilibrium distance of neutral Xe_2 (4.4 Å [21,22]). Therefore, the internuclear distance of Xe_2^+ will remain unchanged as demonstrated in Fig. 3(b) even for longer pulses and will not reach a critical distance for enhanced ionization. Consequently, the kinetic energy of the fragment ions is almost the same as that expected from R_{eq} and does not change by changing τ. In fact, assuming pure Coulombic potentials, two kinetic energy peaks at 1.6 and 3.1 eV shown in Fig. 3(b) correspond to 4.5 and 4.6 Å, respectively, which are close to R_{eq}=4.4 Å of neutral Xe_2. The results shown in Fig. 3(b) also suggest that Xe_2^+ are not produced in their ground state. If so, the internuclear distance will be shortened during the pulse and the released kinetic energy of fragment ions will be increased. However, this is not the case.

Based on the idea of enhanced ionization, the τ dependence of the kinetic energy spectra gives us the following expectations on the angular distributions. The angular distributions of I^+ ions from I_2 molecules elongated by the pulses with a longer τ are expected to appear better aligned along the laser polarization direction, while those of Xe^+ ions are expected to be independent of τ. We evaluate the anisotropy of fragment ions in terms of an anisotropy parameter defined by the ensemble average of cos θ, namely $\langle\langle\cos^2\theta\rangle\rangle$, where θ is the angle between the direction of the laser polarization and that to which the fragment ions are emitted [23]. It is 1/3 for isotropic distribution and 1 for completely anisotropic one. The solid circles in Figs. 5(a) and 5(b) show $\langle\langle\cos^2\theta\rangle\rangle$ obtained for $I^+ + I^+$ and $I^+ + I^{2+}$ channels, respectively, as a function of τ. With the shortest pulses of τ=45 fs, $\langle\langle\cos^2\theta\rangle\rangle$ is ~0.4 for $I^+ + I^+$ and ~0.5 for $I^+ + I^{2+}$. As τ is increased, $\langle\langle\cos^2\theta\rangle\rangle$ gradually increases as expected, and reaches 0.58 and 0.74 for $I^+ + I^+$ and $I^+ + I^{2+}$ channels, respectively, at the longest pulses of τ=660 fs. The increase of $\langle\langle\cos^2\theta\rangle\rangle$ is a corollary of enhanced ionization, which predicts that the fragment distribution becomes more anisotropic as the internuclear distance is elongated and reaches near the critical distance, where the mechanism works efficiently.

As shown in Figs. 2(d)–2(f), the angular distributions of Xe^+ ions are isotropic and expected to be independent of τ. In fact, the anisotropy parameter $\langle\langle\cos^2\theta\rangle\rangle$ for Xe^+ ions [the solid diamonds in Figs. 5(a) and 5(b)] does not show a rapid increase as observed for I^+ ions. The angle dependence of tunnel ionization rates of diatomic molecular species can be estimated by the molecular Ammosov-Delone-Krainov (ADK) theory [24]. We calculate the alignment dependence of the ionization of Xe_2 included as the first step of the production of multiply charged Xe_2^{n+} ($n \geq 2$) and find that the angle dependence of the ionization rate is moderate, which is compatible with rather isotropic distributions of Xe^+ ions shown in Fig. 5 in addition to Figs. 2(d)–2(f) [25]. Looking at Fig. 5 carefully, however, a slight anisotropy is induced as τ is increased both for $Xe^+ + Xe^+$ and for $Xe^+ + Xe^{2+}$ channels. For $Xe^+ + Xe^+$ channel, $\langle\langle\cos^2\theta\rangle\rangle$ increases from 0.33 (random alignment) to 0.35 by increasing τ from 45 to 710 fs, and for $Xe^+ + Xe^{2+}$ channel, it increases from 0.37 to 0.47. The slight increase of $\langle\langle\cos^2\theta\rangle\rangle$ for Xe^+ is most

likely due to the dynamic alignment [26–28] of neutral Xe_2 as discussed below.

In order to estimate the contribution of dynamic alignment, we simulate the degree of alignment by solving the time-dependent Schrödinger equation according to Ref. [26]. We take account of the contribution only from the $|J,M\rangle = |0,0\rangle$ state, which corresponds to the rotational temperature of 0 K. Therefore, the resultant degree of alignment gives us its upper limit, namely $\langle\langle\cos^2\theta\rangle\rangle_{ul}$. The polarizability component perpendicular to the molecular axis $\alpha_\perp$ is assumed to be the same as the polarizability anisotropy $\Delta\alpha \equiv \alpha_\parallel - \alpha_\perp$ [29] ($\alpha_\parallel$ and $\alpha_\perp$ are the polarizability component parallel and perpendicular to the molecular axis, respectively) and the value of $\Delta\alpha$ is taken from Ref. [11]. The solid curve in Fig. 5(a) shows $\langle\langle\cos^2\theta\rangle\rangle_{ul}$ at the peak of the pulses. With the shortest pulses of 45 fs, $\langle\langle\cos^2\theta\rangle\rangle_{ul}$ is ~0.34, indicating that neutral Xe_2 is virtually randomly aligned. As τ is increased, $\langle\langle\cos^2\theta\rangle\rangle_{ul}$ gradually increases. At large τ's, the calculated results overestimate the experimental ones. This is quite reasonable because the nonzero rotational temperature in the experiments and the spatial distribution of the laser pulses are not taken into account in the simulation. Except these overestimates, the simulation reproduces the observed tendency that an anisotropy gradually increases as τ is increased [30]. A steeper increase of the anisotropy observed for $Xe^+ + Xe^{2+}$ channel might be understood by the dynamic alignment of intermediate molecular ions such as Xe_2^+ or Xe_2^{2+}, though we cannot simulate their degrees of alignment because there exists no information about their polarizabilities and we do not know the detailed information about the temporal evolution of (multiple) ionization processes of Xe_2 during the pulses. Furthermore, since the parent Xe_2^{3+} ions are produced at a smaller region with higher intensities in the pulses, the anisotropy observed for $Xe^+ + Xe^{2+}$ should reflect the degree of dynamic alignment at this high-intensity region.

To further investigate the ionization processes of Xe_2, pump-probe experiments will clarify the dependence of the efficacy of enhanced ionization on the internuclear distance as have been demonstrated in the time-of-flight spectra of I_2 molecules [10]. With 293-nm (4.23-eV) pump pulses, for example, the ground state Xe_2 is two-photon excited to 1_g state [Fig. 4(b)] which has a potential minimum at 5.4 Å [31]. By measuring the kinetic energy and the angular distributions of fragment ions as a function of the pump-probe delay, we will be able to know the internuclear-distance dependence of enhanced ionization as well as dynamics of the nuclear motion on the excited potential surface.

IV. CONCLUSIONS

In conclusion, it is demonstrated that Xe_2 is a unique diatomic molecule which shows isotropic fragment distribution under the irradiation of intense femtosecond laser pulses centered at 800 nm. Our recent results suggest that other rare-gas diatomic molecules such as Kr_2 and Ar_2 also belong to the same class of molecules [11]. Compared with Xe_2, the slightly larger anisotropies observed in the angular distributions of fragment ions of Kr_2 and Ar_2 should be reasonably explained by the more efficient dynamic alignment due to their lighter mass or smaller moments of inertia. The present results clearly show that rare-gas diatomic molecules are unexplored samples in the high intensity laser physics.

ACKNOWLEDGMENTS

The authors thank Dr. Tsuneto Kanai for valuable discussions. This work is financially supported by the Grants-in-Aid from Japan Society for the Promotion of Science and Ministry of Education, Culture, Sports, Science and Technology.

[1] See, for example, *Molecules and Clusters in Intense Laser Fields*, edited by J. Posthumus (Cambridge University Press, New York, 2001).
[2] L. J. Frasinski, K. Codling, P. Hatherly, J. Barr, I. N. Ross, and W. T. Toner, Phys. Rev. Lett. **58**, 2424 (1987).
[3] M. Schmidt, D. Norman, and C. Cornaggia, J. Phys. B **25**, L497 (1992).
[4] T. Seideman, M. Yu. Ivanov, and P. B. Corkum, Phys. Rev. Lett. **75**, 2819 (1995).
[5] T. Zuo and A. D. Bandrauk, Phys. Rev. A **52**, R2511 (1995).
[6] E. Constant, H. Stapelfeldt, and P. B. Corkum, Phys. Rev. Lett. **76**, 4140 (1996).
[7] A. Saenz, Phys. Rev. A **61**, 051402(R) (2000).
[8] In the early stage of enhanced ionization studies [4–6], it had been assumed to take place in molecular ions. However, recent theoretical studies reveal that it can occur in neutral molecules as well as in molecular ions based on field-induced curve crossing [7].
[9] V. Véniard, R. Taïeb, and A. Maquet, Phys. Rev. A **65**, 013202 (2001).
[10] Ch. Ellert and P. B. Corkum, Phys. Rev. A **59**, R3170 (1999).
[11] S. Minemoto, H. Tanji, and H. Sakai, J. Chem. Phys. **119**, 7737 (2003).
[12] H. Sakai, S. Minemoto, H. Nanjo, H. Tanji, and T. Suzuki, Phys. Rev. Lett. **90**, 083001 (2003).
[13] S. Minemoto, H. Nanjo, H. Tanji, T. Suzuki, and H. Sakai, J. Chem. Phys. **118**, 4052 (2003).
[14] H. Sakai, S. Minemoto, H. Nanjo, H. Tanji, and T. Suzuki, Eur. Phys. J. D **26**, 33 (2003).
[15] A. T. J. B. Eppin and D. H. Parker, Rev. Sci. Instrum. **68**, 3477 (1997).
[16] M. J. J. Vrakking, Rev. Sci. Instrum. **72**, 4084 (2001).
[17] H. Stapelfeldt, H. Sakai, E. Constant, and P. B. Corkum, Phys. Rev. A **55**, R3319 (1997); Ch. Ellert, H. Stapelfeldt, E. Constant, H. Sakai, J. Wright, D. M. Rayner, and P. B. Corkum, Philos. Trans. R. Soc. London, Ser. A **356**, 329 (1998).
[18] Based on the MP2-level calculation with 3-21G** basis set, we confirm that most of the excited states of I_2^{2+} and Xe_2^{2+} have

repulsive potentials even in the region of small R and approach Coulombic potentials though their ground states have local minima near R_{eq} of the neutral species.
[19] R. S. Mulliken, J. Chem. Phys. **55**, 288 (1971).
[20] R. H. Lipson, P. E. LaRocque, and B. P. Stoicheff, J. Chem. Phys. **82**, 4470 (1985).
[21] K. P. Huber and G. Herzberg, *Molecular Spectra and Molecular Structure. IV. Constants of Diatomic Molecules* (Van Nostrand Reinhold Company, New York, 1979).
[22] R. S. Mulliken, J. Chem. Phys. **52**, 5170 (1970).
[23] In Ref. [26], $\langle\langle\cos^2\theta\rangle\rangle$ denotes the ensemble average of $\cos^2\theta$ while $\langle\cos^2\theta\rangle$ the expectation value of $\cos^2\theta$ for specific J,M values. Here, we use $\langle\langle\cos^2\theta\rangle\rangle$ as the average of $\cos^2\theta$ obtained from the Abel inverted image as has been done in our previous work [11].
[24] X. M. Tong, Z. X. Zhao, and C. D. Lin, Phys. Rev. A **66**, 033402 (2002).
[25] It should be noted that the molecular ADK theory predicts tunneling ionization rates of diatomic molecules under a static electric field and cannot be directly applied to dynamic processes such as enhanced ionization.
[26] J. Ortigoso, M. Rodríguez, M. Gupta, and B. Friedrich, J. Chem. Phys. **110**, 3870 (1999).
[27] F. Rosca-Pruna and M. J. J. Vrakking, Phys. Rev. Lett. **87**, 153902 (2001).
[28] I. V. Litvinyuk, K. F. Lee, P. W. Dooley, D. M. Rayner, D. M. Villeneuve, and P. B. Corkum, Phys. Rev. Lett. **90**, 233003 (2003).
[29] B. Friedrich and D. Herschbach, J. Phys. Chem. A **103**, 10280 (1999).
[30] The present simulations suggest that dynamic alignment should contribute to the increase of $\langle\langle\cos^2\theta\rangle\rangle$ also for $I^+ + I^+$ channel at large τ's at least to some extent.
[31] S. M. Koeckhoven, W. J. Buma, and C. A. de Lange, J. Chem. Phys. **102**, 4020 (1995).
[32] C. R. Scheper, W. J. Buma, and C. A. de Lange, J. Electron Spectrosc. Relat. Phenom. **97**, 147 (1998).